Scanning tunneling spectroscopy on π-conjugated phenyl-based oligomers: A simple physical model

A. I. Onipko, K.-F. Berggren, Yu. O. Klymenko,* and L. I. Malysheva†
Department of Physics, IFM, Linköping University, S-581 83 Linköping, Sweden

J. J. W. M. Rosink, L. J. Geerligs, E. van der Drift, and S. Radelaar‡
Delft Institute of Microelectronics and Submicron Technology and Department of Applied Physics, Delft University of Technology, P.O. Box 5046, 2600 GA Delft, The Netherlands

(Received 25 October 1999)

The current-voltage (I-V) characteristics obtained by scanning tunneling spectroscopy (STS) on uncoated gold substrates and gold substrates coated with self-assembled monolayers of aromatic thiols are shown to be in good quantitative agreement with the Landauer-Büttiker approach to the heterojunction conductance. The self-assembled monolayers consist of one and three chained phenyl rings, forming an azomethine oligomer; both monomer and trimer are chemisorbed on gold via sulphur while terminated from the opposite side by an amine head group. It is found that if the electrostatic energy of the applied potential is ramped within the HOMO-LUMO energy gap (highest occupied molecular orbital-lowest unoccupied molecular orbital) the particular form of the apparent I-V relations reflect an interplay of (i) the WKB factor that accounts for the through-air tunneling between the STM tip and the coated/uncoated substrate, (ii) resonancelike structure of the tip-apex local density of states (LDOS), and (iii) the relative position and intensity of the HOMO and LUMO level peaks in the molecular LDOS. The latter two factors give rise to asymmetry of I-V characteristics. The tunneling spectroscopy measurements and their theoretical evaluation indicate that the STM tip probes a molecular carbon atom rather than the uppermost nitrogen, possibly due to plowing through the molecules. The findings of the work are supported by a close similarity of measured and calculated $I(V)$ curves, which is obtained on different but genetically related samples, at different setpoints of the tunnel current, and with essentially one and the same set of parameters (inferred from experiments and semi-empirical self-consistent modeling of the molecular electronic structure).

I. INTRODUCTION

In this paper, we will investigate electron transport properties in single molecular chains. The study of conductance in such chains is generally complicated by a random molecular orientation and a distribution of chain lengths. In addition, for many experiments the contacts between metal pads and the molecule are ill-defined and cross-linking between chains is not excluded. In contrast, the segment by segment-growth we have pursued (see the experimental part) yields an ordered array of parallel and π-conjugated oligomers, where, in principle, the coupling to the substrate can be known in atomic detail. Above all such a structure would offer the possibility to address individual molecules by making use of a scanning tunneling microscope (STM) tip as a second contact. Since the tunnel current is exponentially decaying with substrate-tip distance, it is reasonable to assume that only one or few molecules are addressed in a current-voltage measurement.

A successful attempt is presented to obtain satisfactory *quantitative* agreement between the theory describing electron transport in metal-molecular heterojunctions and a series of experiments on related molecules performed with one and the same experimental setup. The measurements discussed in this paper refer to both a bare gold substrate and gold substrates covered with a chemisorbed monolayer of a conjugated monomer and respective oligomer (trimer).

A theoretical model used for interpreting experimental results is based on a Green function version of the Landauer-Büttiker approach to the heterojunction conductance (described in detail elsewhere[1]). Unlike previous related experimental-theoretical studies,[2,3] in addition to the molecular electronic structure we also explicitly take into account the tunneling through the gap between the tip and coated/uncoated substrate by means of the WKB approximation. It will be shown that a good correlation can be obtained between the experiment and theoretical estimates of the tip-substrate distance at different setpoints of the tunnel current. This supports the accepted model of the metal-molecular junctions as is described further on.

It is argued that the resonancelike structure of the tip local density of states on one hand and, on the other hand, the identity of a molecular conjugated atom, which is actually probed by the STM tip (not necessarily the outermost one), are playing a crucial role in forming the apparent I-V relation. The agreement between theory and STM spectroscopy experiment on different but related samples is obtained only if both of the above mentioned factors are properly taken into account. The fact that one and the same set of parameters is used to model all molecules is an indication for the strength of the suggested theoretical approach.

II. EXPERIMENT

Gold substrates are prepared as follows: a clean Si(100) wafer is oxidized to obtain a flat SiO_2 layer of about 200 nm

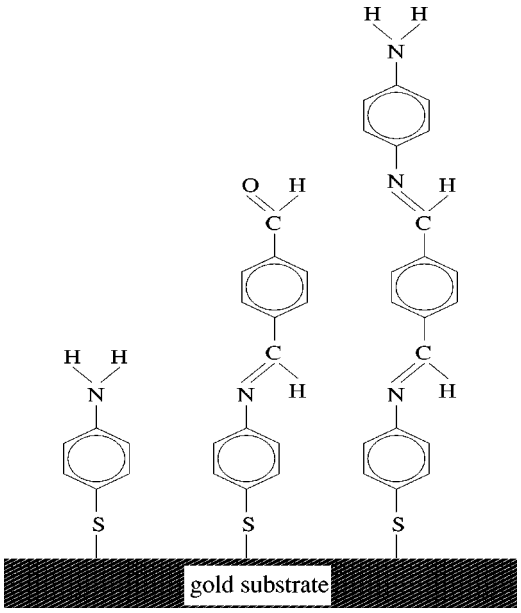

FIG. 1. Schematic picture of the molecules under investigation after their successful growth from solution by self-assembly. From left to right are shown, respectively: 4-ATP (formed by depositing 4-ATP molecules on bare gold substrates), AT (formed by depositing TDA molecules on a thin film of 4-ATP), and ATD (formed by depositing DAB on a thin film of AT).

thickness, and cut afterwards into samples of 6×19 mm. By *e*-beam evaporation, a 100-nm Au film is deposited on top of this layer. The substrates are then annealed in N_2 ambient for 3 hours at 300 °C. This process results in a relatively smooth gold (111) surface with small (50 nm) atomically flat terraces, as evidenced by STM topography measurements.

Gold substrates prepared in this way were used as a starting point to synthesize conjugated oligomers from their constituting monomer building blocks. The molecules containing one central aromatic ring and two functional groups at the para positions were bonding to the substrate by means of a gold-thiol bond or were linking to the monolayers below and above (in the growth process) by means of an imine bond. The monomers were deposited alternately on the gold substrate by making use of *self assembly*: the substrates are immersed in a 10 to 20 mM solution of the organic building blocks in deoxygenated ethanol. Immersion times varying from a few hours up to a day are sufficient to cover the substrate with molecules and let them react with all available surfaces. A detailed analysis of the growth process is given elsewhere.[4] In Fig. 1, the resulting family of the related molecules is shown. In this paper, we will concentrate on 4-ATP and ATD, since they are most similar.

Scanning tunneling microscopy and spectroscopy measurements are done on a Digital Instruments Nanoscope IIIa system with a TipView head using freshly cut $Pt_{0.80}Ir_{0.20}$ tips. All experiments shown here were performed with the specimen in air. Typical tunneling parameters are: bias voltage (V) of 500 mV and tip current of 50 to 500 pA. $I(V)$ data represent the average of 20-50 consecutive $I(V)$ sweeps taken on a gold (111) terrace, at a fixed position on the terrace. Control measurements in nitrogen and on different spots of one and the same sample were also performed. From the collected $I(V)$ curves, only those were included in averaging that were going through (0, 0) and the setpoint. Assuming mostly fluctuations in z as the source of noise in the $I(V)$, we have averaged $\ln(I)$ versus V. The polarity of the bias voltage is defined, in the conventional way, as representing the voltage on the substrate. This means that for negative sample bias voltage electrons tunnel from sample to STM tip.

III. THEORETICAL MODELING AND INTERPRETATION

The total current in a scanning tunneling experiment can be described on the basis of a transfer Hamiltonian formalism developed by Bardeen.[5] Tersoff and Hamman[6] have made the first successful attempt to apply it in the context of an STM set up. In the limit of low temperature and under the assumption of weak STM tip-sample interaction the tunneling current can be expressed as

$$I(V)=I_0\int_{E_F}^{E_F+eV}\rho_s(E)\rho_t(E-eV)\times\exp[-1.025d\sqrt{\Phi+eV/2-(E-E_F)}]dE, \quad (1)$$

where $I_0=(2e/h)\times(\text{e.s.})$; e.s. stands for an appropriate energy scale; under the integral the Fermi energy E_F, the difference in the electron electrostatic energy between the tip and substrate eV, and the metal work function Φ are in units of e.s.; $\rho_s(E)$ is the (dimensionless) local density of states (LDOS), which refers to an atom on the substrate surface which is probed by the STM tip; $\rho_t(E)$ has the same meaning but with regard the tip-apex atom; the exponential factor in Eq. (1), where d is the distance between the substrate and tip (in Angströms) and e.s. is one electron volt, accounts for the through air sample-to-tip tunneling in the WKB approximation.

Equation (1) is equally applicable to describe the electron tunneling between an uncovered metal (bare gold) substrate and STM tip, and when the former is replaced by a substrate with a chemisorbed molecular monolayer. The difference between the substrates used in these experiments has to be properly reflected in a definition of substrate LDOS. We start the discussion from the data obtained on bare gold substrates in which case $\rho_s(E)$ refers to the LDOS of a presumably ideal metal surface.

A. Bare surface gold substrate

Typical experimental I-V curves obtained for bare substrate surfaces are shown in Fig. 2 by filled squares. A noteworthy feature of these data is a systematically larger deviation of the registered current from the Ohm law for negative voltages. This indicates a larger electron current from sample to tip, than that in the opposite direction.

The observed sublinear increase of the current is consistent with an exponential dependence of the tunneling probability on the tunnel barrier height which, as is implied by Eq. (1), is effectively lowered when the applied voltage increases. However, the asymmetry of I-V curves cannot be understood in this way, since the suppression of the potential barrier should be the same for both signs of V, unless the electronic structures of the substrate and tip are not identical.

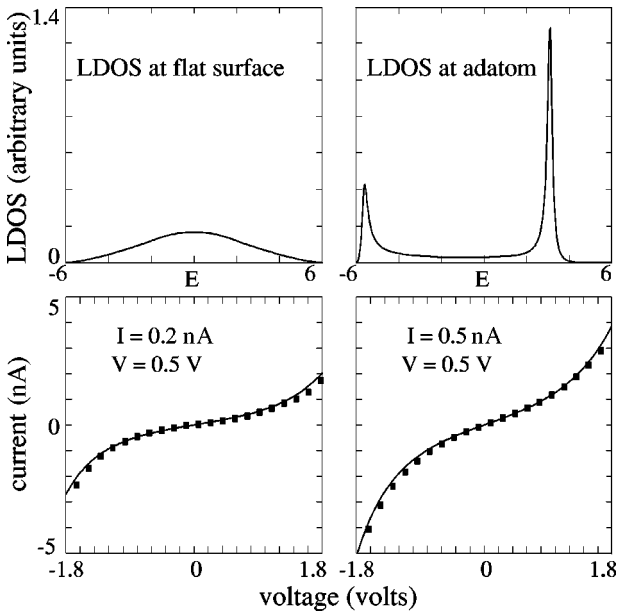

FIG. 2. Upper part: Tight-binding local densities of states at an ideal square lattice surface of semi-infinite cubic crystal [$\rho_s(E)$, to the left] and LDOS of an adatom on such a surface in an on-hollow position [$\rho_t(E)$, to the right]. Lower part: I-V relations (solid lines) are calculated with $\rho_s(E)=\text{const}=0.17$; $\mathcal{V}_a=1.8$, $L=-1$ eV [these parameters determine $\rho_t(E)$]; and the WKB factor with $\Phi=2.2$, $d=7.3$ (left hand side curve), and $d=6.8$ (right hand side curve). In this and other figures, filled square plots represent I on V dependencies measured at two set points as indicated; and $E=0$ corresponds to the Fermi energy of the noninteracting substrate and tip.

According to previous estimates[3] the local density of states at the substrate metal surface is nearly constant. Indeed, if the quality of the metal surface is good enough, there are no physical reasons for a significant variation of the LDOS in the vicinity of the Fermi energy. As an example, the LDOS at a (100) surface of a cubic lattice exhibits a small variation within the range of $E_F\pm 2$ eV (Fig. 2) which has been an actual interval of the electrostatic potential energy in our experiments. So, to model I-V characteristics of the bare gold substrate-STM tip contact, in the first approximation we can neglect the energy dependence of LDOS at a clean metal surface, i.e., in the given case $\rho_s(E)$ is set to be a constant value.

Unlike the substrate metal surface, the quality of which was carefully controlled, the real shape of the ''working part'' of STM tip is never known. It is for sure, however, that it is far from being ideally flat. Therefore, for $\rho_t(E)$ the approximation of a constant LDOS is obviously not applicable.

Here, it is reasonable to use some simple model which accounts for the atomic structure of tip apex. As such we consider an atom placed on the otherwise ideal surface. It is well known[7] that the LDOS at an adsorbed atom may have a pronounced resonancelike structure. The question is at which energy the resonance associated with the presence of an adatom has to be expected?

Suppose for simplicity that an atom is adsorbed in an on-hollow position of a (100) $\mathcal{N}\times\mathcal{N}$ square surface of semi-infinite cubic lattice described by the tight-binding Hamiltonian with the nearest-neighbor hopping integral L. Then, the tip LDOS can be expressed in terms of the effective coupling[1] $A(E)=A^{\mathcal{R}}(E)-iA^{\mathcal{I}}(E)$

$$\rho_t(E)=\frac{1}{\pi}\frac{A^{\mathcal{I}}(E)}{[E-\varepsilon_a-A^{\mathcal{R}}(E)]^2+[A^{\mathcal{I}}(E)]^2}, \tag{2}$$

with the spectral density $A^{\mathcal{I}}(E)$ given by

$$A^{\mathcal{I}}(E)=\frac{64\mathcal{V}_a^2}{(\mathcal{N}+1)^2}\sum_{j_1,j_2=1}^{\mathcal{N}}{}' \sin(k_{j_1,j_2})\sin^2\frac{\pi j_1}{2} \times\sin^2\frac{\pi j_2}{2}\cos^2\frac{\pi j_1}{2(\mathcal{N}+1)}\cos^2\frac{\pi j_2}{2(\mathcal{N}+1)}, \tag{3}$$

where the summation runs over propagating modes only.

In the above equations, e.s.$=|L|$, ε_a is the electron on-site energy at the adatom, $\mathcal{V}_a=L_a/L$, L_a is the hopping integral between the adatom and one of its four nearest neighbors on the metal surface, and k_{j_1,j_2} is related to E by the energy conservation law (in units $|L|$) $E-E_F=-2\{\cos k_{j1,j2}+\cos[\pi j_1/(\mathcal{N}+1)]+\cos[\pi j_2/(\mathcal{N}+1)]\}$; $A^{\mathcal{R}}(E)$ is then determined by the Hilbert transform of $A^{\mathcal{I}}(E)$: $\pi A_a^{\mathcal{R}}(E)=P\int_{-\infty}^{+\infty}A^{\mathcal{I}}(E')/(E-E')dE'$. In calculations we set $\mathcal{N}=50$ that insures $A^{\mathcal{I}}(E)$ to be independent of the transverse dimension. Practically, the convergence to an $A^{\mathcal{I}}(E)$'s constant value is attained at $\mathcal{N}\geqslant 20$.

The distance between the extra atom and its nearest neighbors on the surface is likely to be somewhat smaller than the interatomic distance of the surface square lattice. As a consequence, the corresponding electron hopping integral has to be larger than its counterpart within the supporting surface.

The calculations of Eq. (2) show that, if $\mathcal{V}_a>1$, there are two peaks in the adatom LDOS, see Fig. 2. One of these peaks which is more intense lies above the middle of the tight-binding band determined by the parameter L. The other one is below E_F. The latter is either very weak or (for larger values of $\mathcal{V}_a$) it is far more distant from E_F and also less intensive. Physically, the adatom LDOS resonance structure originates from the adatom electron state (the more pronounced peak) and the electron states of the four surface atoms perturbed by the interaction with the adatom embedded between them.

Thus, the model suggests that there is a peak in the tip LDOS lying close to and above the Fermi energy. An additional argument in support of shifting the resonance upwards is that the apex atom has a smaller number of neighboring atoms to interact and hence, its on-site energy must be somewhat higher.

The LDOS of the apex atom just described gives an explanation of the I-V characteristic asymmetry observed for the bare gold substrate-tip tunnel contact. It is as follows, an increase of the substrate electrochemical potential results in an accompanying increase of the density of unfilled electron states due to approaching to the intense peak of the tip LDOS. Thus, an additional enhancement of the negative current (as is observed in our experiments) has to be regarded as a likely occurrence.

To calculate the I on V dependence (1) with the substrate LDOS $\rho_s(E)=\text{const}$, and tip LDOS as defined above, the zero voltage barrier, i.e., the work function Φ has been de-

duced (of value ≈ 2 eV) from the $I-V$ spectroscopy data obtained in the ohmic regime. The value of I_0 can easily be found from the ohmic slope at a low current, e.g., the set point $I=0.2$ nA, $V=0.5$ V.

As is seen from Fig. 2, with the only fitting parameter $\mathcal{V}_a=1.8$, our model of STM tip LDOS agrees well with experimental data. It is used, therefore, (with an unchanged value of $\Phi=2.2$ eV) in further modeling of tunnel contacts with gold substrates covered by molecular monolayer.

B. I-V characteristics of metal-molecular contacts

In the molecules which are used in these experiments the highest occupied molecular orbital (HOMO) and the lowest unoccupied molecular orbital (LUMO) associate with the π electron states. It is reasonable to assume that just the molecular π electronic subsystem plays a major role in forming the tunnel current between a monolayer-coated substrate and STM tip.

Denoting the molecular (π system) Hamiltonian by $\hat{H}^m$, and the p_z orbitals of the molecular atoms, which are coupled electronically to the substrate and tip, respectively, by $|1\rangle$ and $|N\rangle$, the molecular electronic structure can be included into the substrate local density of states $\rho_s(E)$ as[1]

$$\rho_s(E)=\frac{1}{\pi}\frac{A^{\mathcal{I}}(E)[G^m_{1,N}(E)]^2}{[1-A^{\mathcal{R}}(E)G^m_{1,1}(E)]^2+[A^{\mathcal{I}}(E)G^m_{1,1}(E)]^2}, \tag{4}$$

where the modulus of hopping integral β between phenyl-ring carbons is used as the energy scale (e.s.), $G^m_{1,1(N)}=\langle 1|(E-\hat{H}^m/|\beta|)^{-1}|1(N)\rangle$ is the (dimensionless) matrix element of the molecular Green function, which refers to the states $|1\rangle$ and $|1\rangle$ ($|N\rangle$). Equation (4) implies that sulphur is in the on-hollow position, i.e., that $A^{\mathcal{I}}(E)$ is defined in Eq. (3) with $\mathcal{V}_a$ replaced by $\mathcal{V}_s=L_s/\beta$, L_s has the same meaning as L_a but refers to the sulphur atom.

The π subsystem parameters (see for reference Figs. 3 and 4) which are needed to calculate the LDOS of a molecular monolayer coated substrate, have been found as follows. As a first step, they have been agreed with semi-empirical SCF calculations with the use of the PM3 Hamiltonian for an optimized geometry of the given molecule but without sulphur head group. The values of Hückel parameters indicated in Fig. 4 ensure a remarkably good reproducibility of the SCF results not only for the eigenenergies but also for the full π electronic structure in the molecular ground state, see Table I.

To describe accurately the π subsystem of phenyl-based oligomers headed by a thiol group, the use of the lone atomic orbital approximation for sulphur atom is not sufficient. However, for orientational estimates of the tunnel current it is good enough to use the sulphur parameters that agree with the shift of the HOMO π level, which is produced by a thiol end group attached to the main body of the molecule. As above, the latter effect has been calculated at the PM3 SCF level. The sulphur parameters obtained in this way are represented in Fig. 4. The sulphur-metal coupling constant $\mathcal{V}_s$ has been treated here as a fitting parameter.

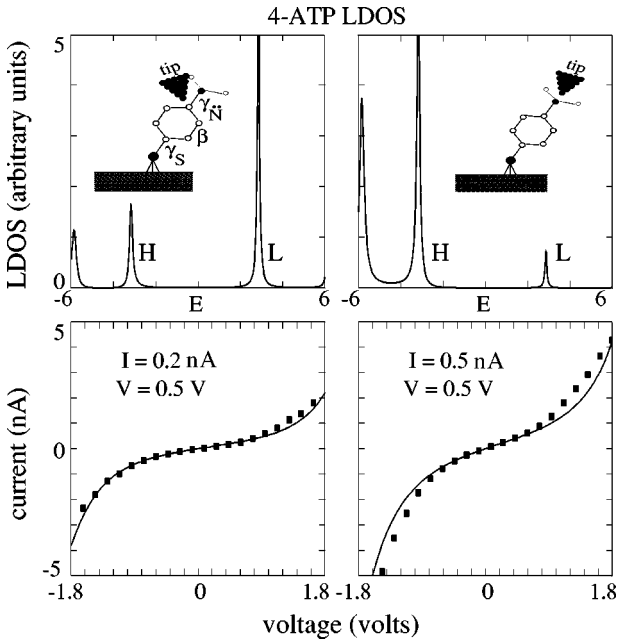

FIG. 3. Upper part: LDOS $[\rho_s(E)]$ at the amine group nitrogen (to the right) and at the neighboring carbon (to the left) of 4-ATP chemisorbed on gold. LDOS at carbon with the parameters: e.s. $=|\beta|=3.5$ eV (see Ref. 8) and those indicated in Fig. 4 was used as $\rho_s(E)$ in Eq. (1) to calculate I-V relations in the lower part of the figure, solid lines. To obtain $I(V)$, we set $\mathcal{V}_s=0.58$ ($\mathcal{V}_a$ is of the same value as in Figs. 2 and 5), the right-hand side maximum of $\rho_t(E)$ is lower in energy by 1.32 eV as compared with Fig. 2, and $d=4.5$ and $d=4$ for, respectively, the smaller and larger current set-points.

1. 4-ATP monolayer

With the system parameters just specified the LDOS (4) calculated at nitrogen and the closest carbon atom of 4-ATP molecule chemisorbed on a substrate is shown in Fig. 3. It is a characteristic feature of this molecule electronic structure that the HOMO and LUMO peaks of LDOS (labeled in the figure as H and L, respectively) have a pronouncedly different intensity. In the nitrogen LDOS the

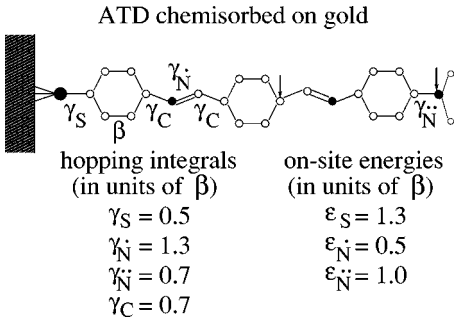

FIG. 4. Schematic structure of the ATD ($=$ HS-C_6H_4-N-CH-C_6H_4-CH-N-C_6H_4-NH_2) molecule (trimer) chemisorbed on gold with an indication of Hückel parameters used to calculate the LDOS at the nitrogen atom of the amine end group and C_4 atom of the second phenyl ring. For the respective monomer (H_5C_6-NH_2) and dimer (H_5C_6-N-CH-C_6H_4-NH_2), the eigenvalues and eigenvectors of the molecular Hamiltonian with the same parameters as given here are represented in Table I.

TABLE I. State labeling (H=HOMO); energies and molecular orbital (MO) coefficients obtained for the PM3 SCF and Hückel Hamiltonians of the molecules H_5C_6-NH_2 and H_5C_6-N-CH-C_6H_4-NH_2. The upper of each pair of lines refers to the SCF calculations. In parentheses, a value is given only if it differs. For the respective trimer an agreement between the PM3 SCF and Hückel models is equally good; the corresponding data are not presented because their volume is too big.

State energy (eV)		Molecule H_5C_6-NH_2 MO coefficients						
		C_1	C_2	C_3	C_4	C_5	C_6	N
H	−8.1	0.43	0.12	−0.36	−0.28	−0.36	0.12	0.66
	−8.3	0.42	0.13	−0.34	−0.35	−0.34	0.13	0.66
H-2	−10.9	−0.50	−0.34	−0.01	0.38	−0.01	−0.34	0.61
	−10.9	−0.48	−0.33	0.02	0.36	0.02	−0.33	0.65
H-3	−13.4	0.31	0.34	0.40	0.51	0.40	0.34	0.32
	−13.4	0.33	0.35	0.40	0.48	0.40	0.35	0.31

State energy (eV)		Molecule H_5C_6-N-CH-C_6H_4-NH_2 MO coefficients										
		First phenyl ring						Second phenyl ring				
		C_1	$C_2(C_6)$	$C_3(C_5)$	C_4	N	C	C_1	$C_2(C_6)$	$C_3(C_5)$	C_4	N
H	−8.4	−0.19	−0.05(−0.08)	0.16(0.15)	0.17	−0.30	−0.18	0.41	0.18	−0.27	−0.33	0.45
	−8.2	−0.18	−0.05	0.15	0.14	−0.30	−0.10	0.46	0.18	−0.36	−0.39	0.69
H-1	−9.5	−0.44	−0.14(−0.25)	0.30(0.21)	0.44	−0.16	−0.32	−0.12	0.06(0.04)	0.20(0.17)	0.09	−0.37
	−9.3	−0.47	−0.21	0.27	0.46	−0.18	−0.31	−0.06	0.08	0.13	0.04	−0.33
H-4	−10.9	0.28	0.18	−0.04(−0.03)	−0.23	−0.32	−0.13	0.35	0.26(0.29)	0.03(0.06)	−0.25	−0.52
	−10.8	0.25	0.16	−0.02	−0.20	−0.31	−0.10	0.39	0.30	0.01	−0.28	−0.57
H-5	−12.2	−0.31	−0.25(−0.26)	−0.12(−0.14)	0.04	0.43	0.45	0.24	0.04	−0.16	−0.33	−0.29
	−12.1	−0.32	−0.28	−0.16	0.01	0.47	0.44	0.21	0.03	−0.16	−0.31	−0.30
H-6	−13.6	−0.24	−0.25(−0.26)	−0.27(−0.29)	−0.33	−0.18	−0.06	0.16	0.19	0.24	0.32	0.19
	−13.4	−0.30	−0.31	−0.35	−0.41	−0.23	−0.06	0.26	0.29	0.34	0.42	0.27
H-7	−14.0	−0.16	−0.18	−0.22(−0.23)	−0.32	−0.34	−0.32	−0.33	−0.25(−0.26)	−0.23(−0.24)	−0.26	−0.13
	−13.8	−0.15	−0.17	−0.22	−0.33	−0.39	−0.34	−0.34	−0.26	−0.24	−0.26	−0.15

HOMO peak is much more intense than its LUMO counterpart. For the LDOS at the α carbon the situation is just reversed.

The above observation is of importance. It indicates that depending on which molecular atom is actually ''probed'' by the STM tip, the current response to the positive and negative tip-sample bias will be substantially different. For example, if the tip sees nitrogen then, from the LDOS consideration the substrate-to-tip current must be larger. Taking also into account the negative current enhancing effect of the tip electronic structure, as discussed above, one has to expect a much stronger nonlinearity of the negative current in the I-V characteristic of 4-ATP samples in comparison with bare gold samples.

However, such an expectation is in obvious conflict with the experimental data represented in Fig. 3. One can see that the presence of the molecular monolayer results in a stronger nonlinearity for both signs of the applied voltage.

To remove the contradiction, we have to admit that the nonlinear increase of the tip-to-sample current is due to an intense LUMO peak in the molecular LDOS. In other words, we assume that the tip is coupled with α carbon more strongly than with nitrogen. The experimental data also suggest that the actual maximum of the tip LDOS has a somewhat lower energy in comparison with the case of bare gold substrate. Then, a good agreement of theory with the observed current response can be obtained under a natural assumption that the Fermi energy of unbiased sample fits the middle of the molecular HOMO-LUMO gap (see caption of Fig. 3 for the values of other fitting parameters).

A point to emphasize is that despite a seemingly large number of the model parameters, theoretical I-V curves cannot agree with experiment unless we accept a stronger tip coupling with the α carbon of phenyl ring, and not with the nitrogen. Such an occurrence cannot be ruled out as nonrealistic, if one takes into account that the average deviation of the molecular axis from the normal to the substrate surface is about 30° and the fact that nitrogen is ''screened'' from the tip by two hydrogens, see insets of Fig. 3.

Thus, according to our model the following three factors are responsible for the current nonlinearity observed on 4-ATP samples: (i) suppressing the tunnel barrier by the applied electric field (the effect is independent of the voltage sign); (ii) the current enhancement due to a more intense LUMO peak and less intense HOMO peak of the molecular LDOS (larger contribution to the positive tip-substrate, than to the negative current); and (iii) the substrate-tip current enhancement due to the tip LDOS peak associated with the tip apex atom. This physical picture is also consistent with the experimental data on ATD-based samples.

2. ATD monolayer

The model molecular Hamiltonian used in these calculations predicts nearly one third decrease of the HOMO-LUMO gap of ATD in comparison with 4-ATP molecule.

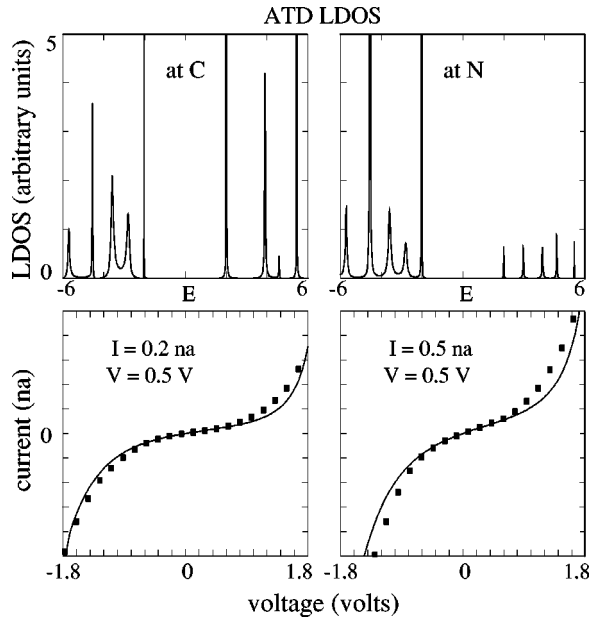

FIG. 5. Same dependencies as in Fig. 3 but $\rho_s(E)$ is at the amine nitrogen and C_4 atom of the second phenyl ring of ATD molecule, see Fig. 4. All parameters are the same as in Fig. 3, except $d=3$ and 2.5 for the smaller and larger current set-points, respectively; and the right-hand side maximum of $\rho_t(E)$ is lower in energy by 1.58 eV as compared with Fig. 2.

This agrees well with a general trend in the dependence of the electronic structure of linear conjugated molecules on the molecular length.[9,10] One would prepare, therefore, to see a much more pronounced nonlinearity of I to V response for samples with a trimer ATD monolayer on gold; at least from the side of a more intense molecular LDOS peak. In fact, the actual nonlinearity increase, which was observed experimentally, turned out to be quite modest; compare the experimental data represented in Figs. 3 and 5. The reason is that, as the molecular electronic levels are approaching each other with the increase of the oligomer length, the LDOS peaks which correspond to these levels are narrowing, see inset Fig. 5. Not surprisingly therefore, that in terms of the molecular ability to transmit electrons, the two effects mentioned above nearly cancel each other.

Furthermore, the current measured on ATD samples is of the same order as that maintained by 4-ATP samples. However, according to Eqs. (1), (2), and (4), if the substrate-molecule coupling constants of these samples do not differ much (both molecules are attached to metal via sulphur and therefore, we do not see any reason for a large difference in the sulphur-metal coupling constants between 4-ATP and ATD samples) then, even at the distance $d=2$ between the tip and ATD terminating nitrogen or next to it carbon atom, the tunnel current must be at least one order of magnitude weaker than that observed experimentally. We have to assume therefore, that the tip sees an atom between the second and the third phenyl rings of the trimer. Again, comparing the calculations with the corresponding experimental data (including a comparison of the molecular length with estimates of a likely distance between the tip apex and substrate metal surface) it was concluded that the atom interacting with the tip apex is C_4 of the second phenyl ring. A reasonable agreement of theoretical curves with experiment, see Fig. 5, supports such a conclusion.

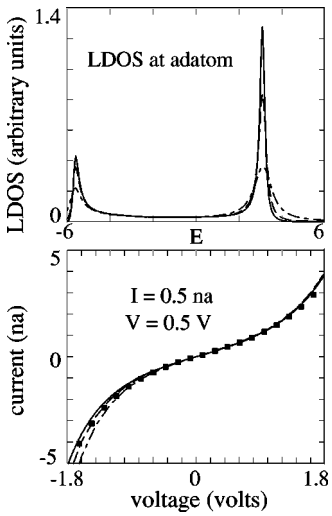

FIG. 6. Comparison of the tip LDOS and I-V relation of Fig. 2 obtained with disregard of inelastic scattering effects with those calculated in the constant energy damping approximation as is explained in the text. Solid, dashed, and dashed-dotted curves correspond to the damping factor equal to zero, 0.01 and 0.05 eV, respectively.

3. Inelastic scattering effects

The physical picture of tunnel current across a molecule spanned between metal electrodes that is developed above does not include energy dissipation effects. In the present context, many likely mechanisms have been discussed in literature.[3,11,12] The basic equation of this analysis has been derived from the exact expression of the ballistic current obtained within the Green function formalism.[1] The latter can be generalized, to take into account the effects of inelastic scattering.[11,13]

Technically, such a generalization may be quite a difficult task, since it requires the precise definition of scattering mechanisms. To avoid unnecessary complications, we use the constant energy damping approximation that proved to give a rough but useful estimate of how the tunnel current can be changed by the electron interaction with phonons and/or other subsystems.

For the purpose, a small imaginary part of the electron energy has been assumed at the level of the exact expression of $I(V)$ in terms of the Green function. As an example, the tip LDOS and the bare gold substrate-STM tip current are represented in Fig. 6 for the different values of damping factor. As expected, the energy dissipation effect suppresses the LDOS peaks and increases their half width. The corresponding effect on the tunnel current is in a clear correlation with these changes of the tip LDOS. A reasonable choice of the damping factor improves the agreement between theory and experiment: for the damping factor of $0.01|L|$ (≈ 0.01 eV) the calculated and measured I-V relations are almost indistinguishable.

IV. CONCLUSION

We have established a model to describe tunneling electron transport through related small conjugated molecules.

We have shown that agreement between experiment and theory can be obtained for these molecules, by only varying the substrate-tip distance, while keeping the different hopping integrals and on-site energies constant. This is a remarkable result which indicates the strength of the model. In order to get agreement with tunneling experiments, it is essential that an appropriate local density of states is used for the tip. Also, the intrinsic molecular properties are important to take into account, since the molecular electron π system governs the tunnel current between the coated substrate and STM tip.

Agreement with ellipsometry experiments on these kind of molecules by Rosink *et al.*[4] was also found. From their thickness measurements it was established that the molecules are tilted slightly with respect to the surface normal. In this paper, it is shown that the tip does not necessarily probe the outermost atoms, but instead that it is likely to be coupled to the C_4 carbon atoms in the first and second aromatic ring of 4-ATP and ATD, respectively. The observation that the tip is apparently not probing the outermost atom of the molecule is possibly due to plowing of the tip through the molecular monolayer, combined with the molecule tilted configuration.

ACKNOWLEDGMENTS

The theoretical part of the work was performed in Linköping under projects of the Swedish Research Council for Engineering Sciences (TFR) and the Royal Swedish Academy of Sciences, Stockholm (KVA). Yu.O.K. wishes to thank the Dutch Science Foundation (NWO) for a supporting grant. L.J.G acknowledges financial support by the Royal Dutch Academy of Sciences (KNAW). The experimental part of this work was performed in Delft as part of the research program of the Dutch Foundation for Fundamental Research of Matter (FOM), which is financially supported by NWO.

*Permanent address: Space Research Institute, Kiev, 252022, Ukraine.

†Permanent address: Bogolyubov Institute for Theoretical Physics, Kiev, 252143, Ukraine.

‡Present address: Netherlands Institute for Metals Research, Rotterdamseweg 137, 2628 AL Delft, The Netherlands.

[1] A. Onipko, Yu. Klymenko, and L. Malysheva (unpublished). A copy of the manuscript is available upon request to: alex@ifm.liu.se; parts of the work are published in A. Onipko, Phys. Rev. B **59**, 9995 (1999) and A. Onipko, Yu. Klymenko, and L. Malysheva, Mater. Sci. Eng., C **8–9**, 273 (1999).

[2] S. Datta, W. Tian, S. Hong, R. Reifenberger, J. I. Henderson, and C. P. Kubiak, Phys. Rev. Lett. **79**, 2530 (1997).

[3] W. Tian, S. Datta, S. Hong, R. Reifenberger, J. I. Henderson, and C. P. Kubiak, J. Chem. Phys. **109**, 2874 (1998).

[4] J. J. W. M. Rosink, M. A. Blauw, L. J. Geerligs, E. van der Drift, W. G. Sloof, S. Radelaar, and E. J. M. Fakkeldij (to be published).

[5] J. Bardeen, Phys. Rev. Lett. **6**, 57 (1961).

[6] J. Tersoff and D. R. Hamman, Phys. Rev. B **31**, 805 (1985).

[7] M.-C. Desjonquéres and D. Spanjaard, *Concepts in Surface Physics* (Springer-Verlag, Berlin, 1993).

[8] This value is close to the value of C-C π hopping integral $\beta = -3.757$ eV deduced experimentally by B. E. Kohler, J. Chem. Phys. **93**, 5838 (1990).

[9] N. Tyutyulkov, J. Fabian, A. Mehlhorn, F. Dietz, and A. Tadjer, *Polymethine Dyes. Structure and Properties* (St. Kliment Ohridski University Press, Sofia, 1991).

[10] A. Onipko, Yu. Klymenko, and L. Malysheva, J. Chem. Phys. **107**, 7331 (1997).

[11] J. Cerdá, M. A. Van Hove, P. Sautet, and M. Salmeron, Phys. Rev. B **56**, 15 885 (1997); **56**, 15 900 (1997).

[12] Z. G. Yu, D. L. Smith, A. Saxena, and A. R. Bishop, Phys. Rev. B **56**, 6494 (1997).

[13] S. Datta, *Electronic Transport in Mesoscopic Systems* (Cambridge University Press, Cambridge, 1995).